

*In Vitro* Cytochrome P450 46A1 (CYP46A1) Activation by Neuroactive Compounds

Natalia Mast<sup>#</sup>, Kyle W. Anderson<sup>‡¶</sup>, Kevin M. Johnson<sup>§</sup>, Thanh T. N. Phan<sup>§</sup>, F. Peter Guengerich<sup>§</sup>,  
and Irina A. Pikuleva<sup>#1</sup>

From the Department of <sup>#</sup>Ophthalmology and Visual Sciences, Case Western Reserve University, Cleveland, OH 44106; <sup>‡</sup>Biomolecular Measurement Division, National Institute of Standards and Technology, Gaithersburg, MD 20899; <sup>¶</sup>Institute for Bioscience and Biotechnology Research, Rockville, MD 20850; and <sup>§</sup>Department of Biochemistry, Vanderbilt University School of Medicine, Nashville, TN 37232.

Running title: *Endogenous CYP46A1 activators*

<sup>1</sup>To whom correspondence should be addressed: Irina A. Pikuleva, Department of Ophthalmology and Visual Sciences, Case Western Reserve University, 2085 Adelbert Rd., Cleveland, OH 44106, Telephone: (216) 368-3823; FAX: (216) 368-0763; E-mail: iap8@case.edu

**Keywords:** CYP46A1, activation, glutamate, brain, cholesterol

Cytochrome P450 46A1 (CYP46A1, cholesterol 24-hydroxylase) is the enzyme responsible for the majority of cholesterol elimination from the brain. Previously, we found that the anti-HIV drug efavirenz (EFV) can pharmacologically activate CYP46A1 in mice. Herein, we investigated whether CYP46A1 could also be activated by endogenous compounds, including major neurotransmitters. *In vitro* experiments with purified recombinant CYP46A1 indicated that CYP46A1 is activated by L-glutamate (L-Glu), L-aspartate,  $\gamma$ -aminobutyric acid, and acetylcholine, with L-Glu eliciting the highest increase (3-fold) in CYP46A1-mediated cholesterol 24-hydroxylation. We also found that L-Glu and other activating neurotransmitters bind to the same site on the CYP46A1 surface, which differs from the EFV-binding site. The other principal differences between EFV and L-Glu in CYP46A1 activation include an apparent lack of L-Glu binding to the P450 active site and different pathways of signal transduction from the allosteric site to the active site. EFV and L-Glu similarly increased the CYP46A1  $k_{cat}$ , the rate of the “fast” phase of the enzyme reduction by the redox partner NADPH-cytochrome P450 oxidoreductase, and the amount of P450 reduced. Spectral titrations with cholesterol, in the presence of EFV or L-Glu, suggest that water displacement from the heme iron can be affected in activator-bound CYP46A1.

Moreover, EFV and L-Glu synergistically activated CYP46A1. Collectively, our *in vitro* data, along with those from previous cell culture and *in vivo* studies by others, suggest that L-Glu-induced CYP46A1 activation is of physiological relevance.

Cytochrome P450 46A1 (CYP46A1) converts cholesterol to 24-hydroxycholesterol (24HC) (1) and thereby initiates the major pathway of cholesterol elimination from the brain (2). Cholesterol 24-hydroxylation is tightly coupled to brain cholesterol biosynthesis (3), the major source of cholesterol for the brain (4). Accordingly, CYP46A1 not only controls the rate of cerebral cholesterol elimination but also the rate of cerebral cholesterol production and the rate of cerebral cholesterol turnover (3). Normally CYP46A1 is expressed in specific neurons of the brain and retina (5, 6), where it resides in the endoplasmic reticulum and requires a source of reducing equivalents (NADPH) along with the redox partner NADPH-cytochrome P450 oxidoreductase (OR), which transfers electrons from NADPH to CYP46A1 (1, 7). In Alzheimer's disease there is also significant CYP46A1 expression in astrocytes and around amyloid plaques, but the reason for this change in the P450 in expression is currently unknown (8, 9). Evidence has accumulated for additional roles of CYP46A1, including involvement in higher order brain functions (10-15) and in processes mitigating

the manifestations of Alzheimer's disease (16-19). Depending on the context, both decreases and increases of CYP46A1 activity have therapeutic potential (14). Hence, we have extensively studied CYP46A1 biochemically and biophysically (7, 20-22) and identified marketed drugs that modulate CYP46A1 activity *in vitro* and *in vivo* (23-25). We have established that CYP46A1-inhibiting drugs (tranylcypromine, thioperamide, clotrimazole, fluvoxamine, bicalutamide, posaconazole, and voriconazole) exert their effects by competing with cholesterol for the enzyme active site, a banana-shaped tunnel extending from the lipid-embedded protein surface to the prosthetic heme group, the site of catalysis (24, 26-29). CYP46A1-activating drugs (efavirenz (EFV), phenacetin, acetaminophen, mirtazapine, and galantamine) act differently, *via* binding to an allosteric site, which is at a distance from the active site and on the cytosolic surface of the molecule; this mechanism was established by studying CYP46A1 activation by EFV, an anti-HIV drug and a representative CYP46A1 activator (25, 30).

In humans, CYP46A1 and 24HC levels reach steady state at ~1 year of age (2-4 weeks of age in mice) and are maintained during adulthood (1, 2, 31). It is also known that *CYP46A1* transcription is insensitive to major regulatory axes, except oxidative stress (32), and may be controlled epigenetically (33-35) as well as by the Sp transcription factors at the level of basal expression (36). Because CYP46A1 can be activated by drugs (25) (i.e., exogenous compounds), we asked whether CYP46A1 could also be activated by endogenous compounds. Such activation could represent a post-translational mechanism of CYP46A1 regulation and would explain *CYP46A1* insensitivity to the major regulatory axes. In addition, this activation could explain a low level of enzyme activity in the reconstituted system *in vitro* (only 0.11 nmol of 24HC formed per nmol of CYP46A1 per min) (21) and link cholesterol 24-hydroxylation to other physiological processes in the brain. Herein, we address the issue of post-translational CYP46A1 regulation by assessing major small molecule neurotransmitters and pertinent neuroactive compounds for their stimulation of cholesterol 24-hydroxylation in an *in vitro* reconstituted system. We demonstrate that several major neurotransmitters can activate purified

recombinant CYP46A1 and bind to an allosteric site that is different from that for EFV. Unexpectedly, CYP46A1 activation was synergistic when EFV and a neuroactivator were simultaneously present in the reconstituted system. Our *in vitro* work is consistent with glutamatergic neurotransmission increasing the CYP46A1-mediated production of 24HC in cultured neurons and mice (37) and allows us to link, in a unifying hypothesis, previously non-associated findings showing the effect of neurotransmission on CYP46A1 (37) and CYP46A1 on neurotransmission (13-15,38).

## Results

### Screening of neuroactive compounds for CYP46A1 activation *in vitro*

CYP46A1 activity was assessed using the truncated  $\Delta(2-50)$  enzyme and reagent concentrations that produce maximal CYP46A1 stimulation by EFV (40  $\mu$ M cholesterol and 20  $\mu$ M neuroactive compound) (25). Under these conditions, five compounds—L-glutamate (L-Glu), L-aspartate (L-Asp), *N*-methyl-D-aspartate (NMDA),  $\gamma$ -aminobutyric acid (GABA), and acetylcholine (ACh)—activated CYP46A1 from 1.5-fold (an arbitrary cut off) to 2-fold (Fig. 1). The effect of truncation on CYP46A1 activation was evaluated by testing the  $\Delta(2-50)$  and  $\Delta(3-27)$  forms. Both truncated forms were activated by neuroactive compounds and showed a similar or even slightly higher activation than full-length CYP46A1 (Fig. 2). Accordingly,  $\Delta(2-50)$ CYP46A1 was used in all subsequent experiments as a more soluble enzyme that also has a higher basal activity.

### Finding cholesterol and neuroactive compound concentrations providing maximal CYP46A1 activation *in vitro*

In the brain, neurotransmitter (e.g., L-Glu) concentrations may vary from 0.5-2  $\mu$ M in the extracellular fluid to  $\geq 100$  mM in synaptic vesicles (39). In the cytoplasm of glutamatergic neurons, the L-Glu concentration is ~5-10 mM and is 2-3 times higher in axon terminals than in cell bodies or dendrites (40). Cholesterol concentrations are

~90  $\mu\text{mol/mg}$  of protein in cerebral cortex microsomes (25), yet the amount available to CYP46A1 is not known. With these considerations in mind, we tested a 20-500  $\mu\text{M}$  range of the neuroactive compound concentrations vs. a 10-40  $\mu\text{M}$  range of cholesterol concentrations for the activating effect on CYP46A1 (Fig. 3). Similar to EFV (25), the maximal neuroactivator effect was observed at a 40  $\mu\text{M}$  cholesterol concentration, which is saturating for CYP46A1, and 20  $\mu\text{M}$  neuroactivator concentration. Only L-Glu required much higher concentrations (100-500  $\mu\text{M}$ ) to maximally activate CYP46A1. Based on these results, 40  $\mu\text{M}$  cholesterol and 100  $\mu\text{M}$  neuroactivator concentrations were selected for use in enzyme assays investigating CYP46A1 activation by neuroactive compounds, and these studies were focused on L-Glu, the strongest CYP46A1 neuroactivator.

CYP46A1 activation by EFV was found to depend on the order in which the components of the reconstituted system were mixed. When EFV was added to the P450 first (prior to the addition of cholesterol), the enzyme activation was ~10-times higher than when EFV was added to CYP46A1 after the addition of cholesterol (25). We tested whether the same results occur with CYP46A1 activation by L-Glu as the representative neuroactivator (Fig. 4). The order of reagent mixing did not have a significant effect on CYP46A1 activation by L-Glu, with the P450 having the same extent of activation regardless of whether it was first mixed with the neuroactivator or cholesterol. This was the first indication of differences in the way EFV and a neuroactivator interact with CYP46A1. Therefore, we investigated how L-Glu affects enzyme kinetics and spectral properties of CYP46A1 and compared these results with those obtained previously for EFV (25).

### **L-Glu effects on the kinetics of cholesterol 24-hydroxylation**

Cholesterol- and OR-dependent kinetics of cholesterol 24-hydroxylation were assessed (Fig. 5). In both cases, L-Glu decreased the  $K_m$  values, 1.8-fold for cholesterol and 2.5-fold for OR, and increased the  $k_{\text{cat}}$  values, 2.5-fold for cholesterol and 3-fold for OR. These effects were different

from those exhibited by EFV, where only  $k_{\text{cat}}$  was increased (~6.7-fold (25)), another piece of evidence supporting different mechanisms of CYP46A1 activation by exogenous and endogenous compounds.

### **Spectral titrations of CYP46A1 with L-Glu and cholesterol**

In the P450 ground state (including CYP46A1), the heme iron is typically six-coordinated and has a water molecule as the sixth axial ligand (21, 41). If a compound (e.g., substrate) displaces this sixth iron ligand to yield a five-coordinated heme iron, a so-called Type I spectral response is observed (42, 43). If a new ligand is coordinated directly to the heme iron, (e.g. the nitrogen atom from a compound), a Type II spectral response is observed (29,30). Thus, changes in the environment of the heme iron enable the determination of the apparent spectral  $K_d$  and the maximal amplitude of the compound-induced P450 spectral response ( $\Delta A_{\text{max}}$ ). Unlike EFV, L-Glu did not elicit a spectral response in CYP46A1 even when very high (1 mM) concentrations were used (Fig. 6A). This could be due either to a lack of L-Glu binding to the CYP46A1 active site or to a lack of water displacement from the heme iron if L-Glu does bind to the P450 active site. Similarly, L-Glu did not induce any spectral changes when CYP46A1 was saturated with 40  $\mu\text{M}$  cholesterol (Fig. 6B), likely because it did not displace cholesterol from the enzyme active site. This response is in contrast to EFV, which induced a Type II spectral response in both cholesterol-free and cholesterol-bound CYP46A1 and showed two-site binding in the presence of cholesterol (25). Reciprocal titrations of CYP46A1 with cholesterol in the presence of 0, 20, 100, and 500  $\mu\text{M}$  L-Glu (Fig. 6C-6F) produced the expected Type I spectral responses and did not significantly affect the apparent  $K_d$  values of cholesterol; only  $\Delta A_{\text{max}}$  values were changed, from 0.07/nmol P450 in the absence of L-Glu to 0.04/nmol P450 in the presence of 500  $\mu\text{M}$  L-Glu. These results indicate that L-Glu does not compete with cholesterol for the CYP46A1 active site and either makes water displacement from the heme iron more difficult or reduces the amount of cholesterol that reaches the CYP46A1 heme iron.

The latter possibility is less likely given the same apparent  $K_d$  values of cholesterol for CYP46A1 in the presence of varying L-Glu concentrations. Collectively, the spectral assay data are consistent with L-Glu binding outside of the CYP46A1 formal active site and inducing changes in the active site that affect water interactions with the heme iron.

### **L-Glu and EFV effects on the kinetics of ferric CYP46A1 reduction by OR**

An increase in  $k_{cat}$  values in the presence of either L-Glu or EFV prompted investigation of CYP46A1 reduction by OR, which sequentially supplies the P450 heme iron with two electrons during the catalytic cycle (44). The rate of CYP46A1 reduction and concentration of reduced P450 were measured under various conditions by trapping the ferrous enzyme as a complex with CO in an anaerobic environment (Table 1). Like some other microsomal P450s (44), CYP46A1 was reduced in the absence of substrate (cholesterol) with the reduction showing biphasic kinetics (Fig. 7). The rate  $k_1$  (for the “fast” phase) was  $0.96 \pm 0.27 \text{ s}^{-1}$  and the rate  $k_2$  (for the “slow” phase) was  $0.060 \pm 0.004 \text{ s}^{-1}$ , with a total of 30% of CYP46A1 being reduced in both phases. In the presence of cholesterol,  $k_1$  was increased,  $k_2$  remained unchanged, and the total amount of reduced P450 increased to 42% because of the increased CYP46A1 reduction in both “fast” and “slow” phases. The reduction rates in the absence and presence of cholesterol were much faster than the  $k_{cat}$  of cholesterol 24-hydroxylation ( $0.11 \text{ nmol of 24HC per nmol of CYP46A1 per min}$ ), suggesting that the first electron transfer step is not rate-limiting in the CYP46A1 catalytic cycle. Similar to cholesterol, L-Glu binding to substrate-free CYP46A1 increased the amount of reduced P450 but did not affect  $k_1$  and  $k_2$ . However, when both L-Glu and cholesterol were present,  $k_1$  was higher than in the separate incubations with cholesterol and L-Glu, as was the amount of reduced CYP46A1;  $k_2$  was not affected. Comparative incubations with EFV added to substrate-free, substrate-bound as well as substrate- and L-Glu-bound CYP46A1 showed the same pattern of changes: a trend to or an increase in  $k_1$ , no change in  $k_2$ , and an increase in the amount of CYP46A1 reduced in the two phases. Thus, both activators

increase the rate of CYP46A1 “fast” reduction and the total amount of reduced P450.

### **L-Glu effects on hydrogen-deuterium exchange (HDX) kinetics of CYP46A1**

HDX kinetics, combined with site-directed mutagenesis, were previously used to identify the CYP46A1 site for EFV binding (30). We applied the same approach to map the site for L-Glu binding and compared deuterium uptake of CYP46A1 in the absence and presence of  $100 \mu\text{M}$  L-Glu. A small but statistically significant difference ( $\Delta D$ ) was detected only in the CYP46A1 region encompassing Thr-88 to Thr-100, which mainly represents the B helix (Fig. 8A,8C) and showed an increase in deuterium uptake upon L-Glu binding. This region, also affected by EFV binding (30), contains Lys-94 and Lys-95, whose positively side chains can potentially interact with the negatively charged L-Glu (Fig. 8B). Therefore, CYP46A1 site-directed mutagenesis was performed to ascertain the meaning of the changes detected by HDX.

### **Site-directed mutagenesis of CYP46A1 and mapping of the CYP46A1 site for Glu binding**

Three sets of amino acid residues were ultimately selected for evaluation of their involvement in L-Glu binding, all in the same region on the cytosolic side of CYP46A1 (Fig. 8B). These were Lys-94 and Lys-95 (suggested by differential HDX), Lys-422 and Arg-424 (investigated previously for EFV binding (30)), and Lys-358, Arg-415, Phe-416, and Tyr-427 (located in the CYP46A1 surface trough near the site of EFV binding). The K94A, K94L, K95A, and K95L replacements could not be assessed because they led to inactive cytochrome P420 protein; all other mutants were expressed and purified. Of these, only the Lys-358A, Phe-416A, and Tyr-427A mutants were not activated by L-Glu (Fig. 9A). These were the replacements of the residues whose side chains are all in proximity to each other (Fig. 9B), forming a pocket defined by the parts of the K' and L helices along with the K'-L loop. Computational docking of L-Glu to the CYP46A1 surface was then carried out and produced multiple models for neurotransmitter binding, including that requiring Lys-358, Phe-



416, and Tyr-427 (Fig. 9B). In this model, the L-Glu O4 forms a polar contact with the Lys-358 amino group, whereas the L-Glu C5, C4, and C3 atoms are constrained by the side chains of Phe-416 and Tyr-427 (Fig. 9B). Site-directed mutagenesis data supported this model (Fig. 9A), suggesting that we did map the site for L-Glu binding, which is different from that for EFV binding (Fig. 9B). The D stereoisomer of glutamic acid (D-Glu) was then tested for activation of CYP46A1 and was found to increase the CYP46A1 activity to the same extent as L-Glu (Fig. 9A). Computational docking of D-Glu to the CYP46A1 surface showed that this stereoisomer can interact with the same allosteric site as L-Glu yet have a different binding pose (Fig. 9C). Remarkably, in this binding pose, D-Glu interacts with same set of amino acid residues in CYP46A1 (Lys-358, Phe-416, and Tyr-427) as L-Glu, consistent with the site directed-mutagenesis data (Fig. 9A). Experiments were next performed to further address the hypothesis that CYP46A1 has different binding sites for EFV and Glu.

### CYP46A1 interactions with Glu and EFV

The CYP46A1 mutations that were evaluated for activation by L- and D-Glu were also evaluated for activation by EFV (Fig. 9A). None of the mutations that abolished CYP46A1 activation by Glu (Lys-358A, Phe-416A, and Tyr-427A) eliminated EFV binding and, *vice versa*, the two mutations that abolished CYP46A1 activation by EFV (the Arg-415A and Arg-424A) preserved Glu activation. These differential effects of mutations provide additional support for distinct sites of binding of Glu and EFV on CYP46A1. We incubated CYP46A1 with both EFV and L-Glu simultaneously and found higher enzyme activation than in the separate incubations with the two activators alone (Fig. 4). Finally, we investigated the effects of ionic strength and the non-ionic detergent CYMAL-6 on CYP46A1 activation by L-Glu and EFV (Fig. 10). Increasing the ionic strength to 600-900 mM NaCl abolished CYP46A1 activation by L-Glu but had a much lesser effect on CYP46A1 activation by EFV (Fig. 10A). Conversely, increasing the concentration of CYMAL-6 to 0.04% (w/v) abolished CYP46A1 activation by EFV and had a minor effect on activation by L-Glu. Thus, electrostatic

interactions are important for CYP46A1 activation by L-Glu, whereas hydrophobic interactions are important for EFV effects. These data are consistent with the polar nature of Glu and the role of Lys-358 in Glu activation. They also support the putative mode of EFV binding (Fig. 9B) and hydrophobic interactions within this allosteric site defined by the K'-K'' and K''-L loops and the K'' helix (30).

### Effect of mutations on CYP46A1 activation by neuroactivators other than Glu

All neuroactive compounds that activate CYP46A1 *in vitro*, at physiological pH, appear to share some structural similarities such as a flexible aliphatic chain carrying an amine group and either a partial (Ach) or at least one full negative charge (Glu, Asp, NMDA, kainic acid, and GABA) (Fig. 11). Hence, like Glu, they can potentially interact with Lys-358, which is involved in Glu binding. The CYP46A1 mutations at Lys-358 were tested, as well as at the other amino acid residues (Fig. 11), and we found that only those that abolished CYP46A1 activation by Glu abolished P450 activation by other neuroactive compounds. These results suggest that all neuroactivators tested have a common binding site on the CYP46A1 surface, consistent with their structural similarity and the presence of a negatively charged functionality. Only the Y427A mutant was slightly activated by Ach, consistent with the lack of a second negatively charged functionality.

### Discussion

The present work revealed that not only drugs but also endogenous compounds, namely some of the major neurotransmitters, can activate CYP46A1 *in vitro*. Neuroactivators were found to bind to a different CYP46A1 allosteric site (Fig. 9) and share with EFV both similarities and differences in the way that they activate this P450. The shared similarities include a common region (B helix) showing a change in deuterium uptake upon binding—a decrease in  $\Delta D$  in the case of EFV and an increase in  $\Delta D$  in the case of L-Glu. Also, both activator types increased the rate ( $k_{cat}$ ) for the CYP46A1-mediated catalysis (Fig. 5) and the rate ( $k_1$ ) of the P450 reduction by the redox partner OR (Table 1). In addition, they increased

the amount of CYP46A1 reduced by OR (Table 1) but decreased the maximal amplitude of the activator-induced P450 spectral response ( $\Delta A_{\max}$ ) (Fig. 6C-F). All these changes are consistent with the activator-induced signal transduction involving a CYP46A1 hydrogen bond network and subsequent changes in the hydration of the enzyme active site. Previously, we proposed that EFV binding displaces one or more water molecules in the allosteric site and thereby alters the hydrogen bond network connecting the allosteric site and the enzyme active site (30). Similarly, our computational docking of L-Glu suggests that at least five water molecules (W703, W760, W773, W777, and W827) could be displaced by L-Glu binding and thereby alter two hydrogen bond networks (Fig. 12A). One network includes the N-terminal part of the K'-L loop and the B-helix, which showed an increase in deuterium uptake upon L-Glu binding. The other network is formed by the L helix and the C-terminal part of the K'-L loop, which did not show any changes in  $\Delta D$ . The L helix and K'-L loop define the sides of the CYP46A1 active site proximal to the heme group (i.e. below this group), which encompasses C437 serving as the fifth ligand to the heme iron. In addition to the coordination of the heme iron, Cys-437 is also hydrogen bonded to W734, which is a part of the L-helix hydrogen bond network and which can be affected by L-Glu displacement of W760 and W773. Thus, L-Glu binding can alter the Cys-437 ligation of the heme iron and in turn affect W732 serving as the sixth heme ligand. The latter could make the W732 displacement by cholesterol more difficult and be manifested in the  $\Delta A_{\max}$  decrease. In addition, the W760 and W773 displacements can alter the hydration of the proximal part of the CYP46A1 active site containing W779 and W701, which are within 3.6 Å from W734 and the L helix Gln-440 side chain. Changes in the active site hydration can explain the alterations in the CYP46A1  $k_{\text{cat}}$ ,  $k_i$ , and the amount of reduced CYP46A1, although more proof is in order. Like L-Glu, D-Glu can also displace W777, W798, W827, and W741 upon binding and alter the same two hydrogen bond networks that are affected by the L-Glu binding (data not shown).

The differences in the CYP46A1 activation by EFV and Glu include binding to the distinct allosteric sites on the protein surface (Fig. 9), EFV

but not Glu binding to the CYP46A1 active site when present at high concentrations (30), L-Glu but not EFV effects on  $K_m$  for OR (Fig. 5), and the lack of importance of the reagent mixing order in the case of L-Glu (Fig. 4). Our previous findings provide explanations for the latter two differences. Glu seems to bind in the trough on the surface that is also the site of OR binding (Fig. 12B) (30). Perhaps Glu fills this trough and increases the CYP46A1 complementarity to the OR surface, thus decreasing the CYP46A1-OR  $K_d$ . As far as reagent mixing order, EFV decreases the deuterium uptake of the regions defining the distal (above the heme) portion of the CYP46A1 active site, i.e. the site where cholesterol binds and catalysis takes place. These decreases in  $\Delta D$  suggest conformation changes in the CYP46A1 active site, which did not seem to occur upon Glu binding. The active site of substrate-free CYP46A1 is likely to be more flexible than the active site of cholesterol-bound CYP46A1. Hence, EFV activates CYP46A1 to a much greater extent when it is added to substrate-free enzyme. EFV effects on both distal and proximal parts of the CYP46A1 active site, and Glu effects on the proximal part of the active site may explain synergistic CYP46A1 activation in the presence of both activators.

CYP46A1 activation by different neurotransmitters *in vitro*, including the glutamatergic ones, is consistent with cell culture and *in vivo* treatments investigating the effect of glutamate-mediated excitotoxicity on neuronal cholesterol (37). In these experiments, excessive stimulation of glutamate receptors either by NMDA (added to cultured hippocampal neurons) or kainic acid (injected into mice) led to a loss of membrane cholesterol and, in the former case, to a parallel extracellular release of 24HC (37). Immunogold labeling (followed by electron microscopy) detected CYP46A1 in both endoplasmic reticulum and plasma membranes of mouse hippocampal dendritic spines, with more CYP46A1 being associated with plasma membranes in kainic acid-injected vs saline-injected mice. Accordingly, excitatory neurotransmission was suggested to mobilize CYP46A1 from the endoplasmic reticulum (where it mainly resides (5)) towards the plasma membranes to convert some of the cholesterol there to 24HC (37). CYP46A1-mediated

cholesterol 24-hydroxylation requires OR and NADPH, which were not investigated in this work for their presence in the plasma membranes of postsynaptic neurons and synaptic space, respectively. Hence, the data obtained could have an additional explanation based on our findings, the millimolar L-Glu concentrations in the cell bodies and dendrites of glutamatergic neurons (40), and CYP46A1 localization in the cell bodies and dendrites in multiple neuron types in the hippocampus and cortex (5).

We suggest that *in vivo* CYP46A1 could be activated by L-Glu intraneuronally, and this activation serve as a post-translational mechanism of regulation of CYP46A1 activity. Furthermore, in Alzheimer's disease, CYP46A1 expression is detected in astrocytes (8,9), which take up L-Glu from the synaptic space to convert it to glutamine. Thus, it is plausible that under certain conditions, CYP46A1 may be activated by L-Glu in astrocytes as well. Currently studies by others (37) and the present work strongly support the neurotransmission to CYP46A1 activity link. Intriguingly, the reciprocal CYP46A1 activity to neuroreceptor link was also recently established by showing that the CYP46A1 metabolite 24HC is a potent positive allosteric modulator of NMDAR activity in primary hippocampal neurons, excised membrane patches, and recombinant NMDAR (13, 15, 45). 24HC was found to bind to the NMDAR site, distinct from other modulators, and to access this site from the extracellular side of the plasma membrane (13). The latter finding indicates that, prior to NMDAR binding, 24HC has to be released from the cell of origin (45), consistent with the rapid 24HC diffusion from the cells once it is formed (46). Hence, we propose that there may be a reciprocal relationship between CYP46A1 activity and neurotransmission: excitatory neurotransmission increases CYP46A1 activity, and increased CYP46A1 activity enhances neurotransmission, with both processes being regulated by the same compounds, namely L-Glu and 24HC. Experiments testing this hypothesis, as well as *in vivo* relevance of our *in vitro* findings, are in progress.

In summary, CYP46A1 activation by neurotransmitters was investigated *in vitro* and compared to that by exogenous compounds. Both similarities and differences were found in the mechanism of CYP46A1 activation by xeno- and

endobiotics. On the basis of the data obtained, as well as previous studies by others (13, 15, 37, 45), we suggest that CYP46A1 activation by the major excitatory neurotransmitter L-Glu may be of physiological relevance and that there may be a reciprocal relationship between CYP46A1 activity and neurotransmission and, *vice versa*, neurotransmission and CYP46A1 activity.

## Experimental Procedures

### Materials

L- and D-Glu, L-Asp, NMDA, kainic acid, GABA, Ach, D-serine, glycine, pregnenolone sulfate, histamine, memantine, quisqualic acid, aniracetam, epinephrine, norepinephrine, dopamine, serotonin, and carbachole were from Sigma-Aldrich. The (S)-isomer of EFV (brand name Sustiva) was purchased from Toronto Research Chemicals (Toronto, ON, Canada). Cholesterol was obtained from Steraloids (Newport, RI). Neuroactive compounds were added from 2 mM stocks in water (Glu, L-Asp, NMDA, kainic acid, GABA, Ach, D-serine, glycine, histamine, quisqualic acid, dopamine, serotonin, and carbachole) or 2 mM stocks in methanol (pregnenolone sulfate, memantine, aniracetam, epinephrine, and norepinephrine). EFV was dissolved in methanol and added from 0.5-10 mM stocks. Cholesterol was added from 0.5-10 mM stocks in 4.5 to 45% (w/v) aqueous 2-hydroxypropyl- $\beta$ -cyclodextrin. Full-length CYP46A1,  $\Delta(3-27)$ CYP46A1, and  $\Delta(2-50)$ CYP46A1, all with a four-histidine tag on the C-terminus, were expressed in *Escherichia coli* and purified as described (20, 47). Rat OR was also expressed in *E. coli* and purified as described (48).

### Screening enzyme assay for CYP46A1 activation by different compounds

The conditions of the assay were as described (25), with the following reagent concentrations: 50 mM KPi (pH 7.2), 100 mM NaCl, 40  $\mu$ g/ml L- $\alpha$ -1,2-dilauroyl-*sn*-glycero-3-phosphocholine, 0.5  $\mu$ M purified  $\Delta(2-50)$ CYP46A1, 1.0  $\mu$ M OR, 40  $\mu$ M cholesterol, 20  $\mu$ M of each test compound, 2 units of catalase, and an NADPH-regenerating system (1 mM NADPH, 10 mM glucose-6-

phosphate, and 2 units of glucose-6-phosphate dehydrogenase). After a 30-min incubation at 37 °C, sterols were extracted by dichloromethane supplemented with 1 nmol of 24-hydroxy-[25,26,26,26,27,27,27-<sup>2</sup>H<sub>7</sub>]-cholesterol, serving as an internal standard. Sterol extracts were analyzed by gas chromatography-mass spectrometry (49).

### Effect of truncation on CYP46A1 activation by Glu

Individual enzyme assays with full-length CYP46A1, Δ(3-27)CYP46A1, and Δ(2-50)CYP46A1 were as above, except that incubations with full-length CYP46A1 contained 0.02% CYMAL-6 (w/v).

### Screening of the conditions for maximal CYP46A1 activation by neuroactive compounds

The conditions were identical to those used in the screening enzyme assays, except that cholesterol and neuroactivator concentrations were varied from 10 to 40 μM and from 0 to 500 μM, respectively.

### Kinetic Parameters for Cholesterol and OR

These were determined by measuring the rates of cholesterol 24-hydroxylation by Δ(2-50)CYP46A1 at constant P450 (0.5 μM) and varying cholesterol (0-80 μM) or OR (0-10 μM) concentrations. When cholesterol concentrations were varied, the OR concentration was 1 μM. When OR concentrations varied, the cholesterol concentration was 20 μM. All other conditions were identical to those of the screening enzyme assay. 24HC formation was linear with time and CYP46A1 concentration. *K<sub>m</sub>* and *k<sub>cat</sub>* values of cholesterol and OR for CYP46A1 were calculated with Prism software (GraphPad Software, San Diego, CA) using the Michaelis–Menten equation and non-linear regression.

### Spectral Binding Assay

Spectral titrations were carried out at 24 °C as described (29), namely, in 1 ml of 50 mM KPi buffer (pH 7.2) containing 100 mM NaCl and 0.3 μM Δ(2-50)CYP46A1. Stock solutions of 10-50 mM L-Glu in water or 0.5 mM cholesterol in 4.5%

(w/v) aqueous 2-hydroxypropyl-β-cyclodextrin were used. Apparent binding constants (*K<sub>d</sub>*) were calculated using either the  $\Delta A = (\Delta A_{\max}[L]/(K_d + [L]))$  or

$$\Delta A = 0.5 \Delta A_{\max} (K_d + [E] + [L] - \sqrt{(K_d + [E] + [L])^2 - 4[E][L]})$$
 equations, in which *E* is the enzyme concentration; Δ*A* is the spectral response at different ligand (sterol) concentrations [*L*], and Δ*A<sub>max</sub>* is the maximal amplitude of the spectral response.

### Stopped-Flow Experiments

Anaerobic kinetic experiments were conducted by loading the stopped-flow instrument (OLIS RSM-1000, On-Line Instrument Systems, Bogart, GA) with samples from all-glass tonometers that had been degassed and placed under a CO atmosphere as described in more detail elsewhere (50-52). The syringes of the stopped-flow apparatus had previously been scrubbed with an anaerobic solution of a mixture of protocatechuate dioxygenase (62 mU ml<sup>-1</sup>) and 3,4-dihydroxybenzoic acid (0.25 mM) (53, 54). Assays were done by mixing the contents of two syringes in a stopped-flow spectrophotometer at 37 °C. One syringe contained 3 μM Δ(2-50)P450 46A1, 6 μM OR, 40 μM L-α-1,2-dilauroyl-*sn*-glycero-3-phosphocholine, and 100 mM NaCl. In addition, cholesterol (40 μM), L-Glu (100 μM), and EFV (20 μM) were added as noted. The other syringe contained 0.40 mM NADPH. Both syringes contained 50 mM KPi (pH 7.4) buffer and 62 mU ml<sup>-1</sup> protocatechuate dioxygenase and 0.25 mM 3,4-dihydroxybenzoic acid. Scans (375-525 nm) were collected over 60 seconds or, in some cases, 4 seconds (no *k<sub>2</sub>* calculations were done with the 4-second data). The data were fit as biphasic first-order processes (55) using SVD fitting (OLIS GlobalWorks) to obtain rates (mean of 3-17 experiments in each case). We found the best fitting with single exponentials applied to two different data sets: 0-2 s for *k<sub>1</sub>* and 4-60 s for *k<sub>2</sub>*.

### HDX

Sample preparation, LC-MS, data acquisition, and HDX-MS analyses were carried out as described (30). Briefly, two samples of 4 μM Δ(2-50)CYP46A1 in 50 mM KPi buffer (pH 7.2)



containing 100 mM NaCl were prepared: CYP46A1 only and CYP46A1 with 100  $\mu$ M L-Glu. Samples (final volume 1.0 ml) were incubated for 15 min at room temperature to establish binding equilibrium and then stored prior to analysis in the autosampler, which was maintained at 1 °C. A fully-automated HDX PAL robot (LEAP Technologies, Carrboro, NC) was used to carry out sample labeling, quenching, inline proteolysis, desalting, and analytical separation. This robot was coupled to a Thermo LTQ Velos Orbitrap Elite mass spectrometer (Thermo Fisher, San Jose, CA). Protein samples (a total of 5  $\mu$ l) were diluted by the PAL robot into 21  $\mu$ l of D<sub>2</sub>O buffer (50 mM KPi buffer (pD 7.2) containing 100 mM NaCl), and HDX was performed at 25 °C in triplicate for 30 s, 1 min, 5 min, 15 min, and 1 h exchange times. CYP46A1 samples in undeuterated buffer served as 0 s controls. Exchange reactions were quenched by addition of 35  $\mu$ l of 3 M urea and 100 mM sodium phosphate (pH 2.5) at 1 °C, followed by digestion for 3 min in-line with an immobilized pepsin column (Enzymate BEH, 2.1 mm  $\times$  30 mm, 5  $\mu$ m, Waters, Milford, MA). Peptide digests were loaded onto a C<sub>18</sub> guard column (1.0 mm, 5  $\mu$ m, Grace Discovery Sciences) for desalting followed by separation on a Dionex Ultimate 3000 UPLC with a C<sub>18</sub> Hypersil GOLD analytical column (1.0 mm  $\times$  5 cm, 1.9  $\mu$ m, Thermo Scientific). Peptide analysis was performed on the Orbitrap of a Thermo LTQ Velos Orbitrap Elite. Peptides were identified by MASCOT (Matrix Science, Oxford, UK), and their amino acid sequences and associated retention times were imported into HDX WorkBench (Scripps Research Institute, Jupiter, FL) (56). HDX WorkBench calculated D% using the following equation (57):  $D\% = \frac{[m(\text{partially deuterated}) - m(\text{undeuterated})]}{[m(\text{fully deuterated}) - m(\text{undeuterated})]} \times 100\%$ ; and also generated kinetic plots of deuterium uptake with each plotted

data point representing an average of triplicate measurements.

### Computational predictions of Glu binding on the CYP46A1 surface

The web-based SwissDock program (58) was used to dock the L- and D-isomers of Glu to cholesterol sulfate-bound CYP46A1 (PDB code 2Q9F). The docking was performed using the default parameters with no region of interest defined (blind docking).

### Site-directed mutagenesis and enzyme assay with mutant P450s

The mutations were introduced into the  $\Delta(2-50)$ CYP46A1 expression construct (47) using an *in vitro* QuikChange site-directed mutagenesis kit (Stratagene) according to the instructions. The correct generation of desired mutations and the absence of undesired mutations were confirmed by DNA sequencing of the entire CYP46A1 coding region as well as by the restriction analysis. The mutant P450s were heterologously expressed in *E. coli* and purified as described (47). Enzyme assay was the same as in the screening assay, except that the neuroactivator concentration was 100  $\mu$ M.

### Data Analysis

All results are presented as means  $\pm$  S.D. All *in vitro* assays were carried out at least in triplicate. Statistical significance of mean differences was determined either by a 2-tailed, unpaired Student's *t* test or by repeated measures two-way ANOVA followed by a *post hoc* Bonferroni multiple comparison test. The significance is defined as \*,  $p \leq 0.05$ ; \*\*,  $p \leq 0.01$ ; and \*\*\*,  $p \leq 0.001$ . All statistical analyses were performed using either GraphPad Prism (GraphPad Software, SanDiego, CA) or HDX WorkBench software.

**Acknowledgements:** The authors thank John Denker from the NEI P30 Molecular Biology and Genotyping Core for the generation of the CYP46A1 mutants at the DNA level.

**Conflict of interest:** The authors have declared that no conflict of interest exists.

**Author contributions:** N. M., K. W. A., K. M. J., T. T. N. P., and F. P. G. conducted experiments, N. M., K. W. A., K. M. J., F. P. G., and I. A. P. analyzed the data; N. M. and I. A. P. designed experiments; and I. A. P. wrote the manuscript.

## References

1. Lund, E. G., Guileyardo, J. M., and Russell, D. W. (1999) cDNA cloning of cholesterol 24-hydroxylase, a mediator of cholesterol homeostasis in the brain. *Proc. Natl. Acad. Sci. U. S. A.* **96**, 7238-7243
2. Lutjohann, D., Breuer, O., Ahlborg, G., Nennesmo, I., Siden, A., Diczfalusy, U., and Björkhem, I. (1996) Cholesterol homeostasis in human brain: evidence for an age-dependent flux of 24S-hydroxycholesterol from the brain into the circulation. *Proc. Natl. Acad. Sci. U. S. A.* **93**, 9799-9804
3. Lund, E. G., Xie, C., Kotti, T., Turley, S. D., Dietschy, J. M., and Russell, D. W. (2003) Knockout of the cholesterol 24-hydroxylase gene in mice reveals a brain-specific mechanism of cholesterol turnover. *J. Biol. Chem.* **278**, 22980-22988
4. Dietschy, J. M., and Turley, S. D. (2001) Cholesterol metabolism in the brain. *Curr. Opin. Lipidol.* **12**, 105-112
5. Ramirez, D. M., Andersson, S., and Russell, D. W. (2008) Neuronal expression and subcellular localization of cholesterol 24-hydroxylase in the mouse brain. *J. Comp. Neurol.* **507**, 1676-1693
6. Bretillon, L., Diczfalusy, U., Bjorkhem, I., Maire, M. A., Martine, L., Joffre, C., Acar, N., Bron, A., and Creuzot-Garcher, C. (2007) Cholesterol-24S-hydroxylase (CYP46A1) is specifically expressed in neurons of the neural retina. *Curr. Eye Res.* **32**, 361-366
7. Mast, N., Norcross, R., Andersson, U., Shou, M., Nakayama, K., Bjorkhem, I., and Pikuleva, I. A. (2003) Broad substrate specificity of human cytochrome P450 46A1 which initiates cholesterol degradation in the brain. *Biochemistry* **42**, 14284-14292
8. Bogdanovic, N., Bretillon, L., Lund, E. G., Diczfalusy, U., Lannfelt, L., Winblad, B., Russell, D. W., and Bjorkhem, I. (2001) On the turnover of brain cholesterol in patients with Alzheimer's disease. Abnormal induction of the cholesterol-catabolic enzyme CYP46 in glial cells. *Neurosci. Lett.* **314**, 45-48
9. Brown, J., 3rd, Theisler, C., Silberman, S., Magnuson, D., Gottardi-Littell, N., Lee, J. M., Yager, D., Crowley, J., Sambamurti, K., Rahman, M. M., Reiss, A. B., Eckman, C. B., and Wolozin, B. (2004) Differential expression of cholesterol hydroxylases in Alzheimer's disease. *J. Biol. Chem.* **279**, 34674-34681
10. Kotti, T. J., Ramirez, D. M., Pfeiffer, B. E., Huber, K. M., and Russell, D. W. (2006) Brain cholesterol turnover required for geranylgeraniol production and learning in mice. *Proc. Natl. Acad. Sci. U. S. A.* **103**, 3869-3874
11. Kotti, T., Head, D. D., McKenna, C. E., and Russell, D. W. (2008) Biphasic requirement for geranylgeraniol in hippocampal long-term potentiation. *Proc. Natl. Acad. Sci. U S A* **105**, 11394-11399
12. Maioli, S., Bavner, A., Ali, Z., Heverin, M., Ismail, M. A., Puerta, E., Olin, M., Saeed, A., Shafaati, M., Parini, P., Cedazo-Minguez, A., and Björkhem, I. (2013) Is it possible to improve memory function by upregulation of the cholesterol 24S-hydroxylase (CYP46A1) in the brain? *PLoS One* **8**, e68534-e68534
13. Paul, S. M., Doherty, J. J., Robichaud, A. J., Belfort, G. M., Chow, B. Y., Hammond, R. S., Crawford, D. C., Linsenhardt, A. J., Shu, H. J., Izumi, Y., Mennerick, S. J., and Zorumski, C. F. (2013) The major brain cholesterol metabolite 24(S)-hydroxycholesterol is a potent allosteric modulator of N-methyl-D-aspartate receptors. *J. Neurosci.* **33**, 17290-17300
14. Sun, M. Y., Linsenhardt, A. J., Emnett, C. M., Eisenman, L. N., Izumi, Y., Zorumski, C. F., and Mennerick, S. (2016) 24(S)-Hydroxycholesterol as a modulator of neuronal signaling and survival. *Neuroscientist* **22**, 132-144

15. Sun, M. Y., Izumi, Y., Benz, A., Zorumski, C. F., and Mennerick, S. (2016) Endogenous 24S-Hydroxycholesterol modulates NMDAR-mediated function in hippocampal slices. *J. Neurophysiol.* **115**, 1263-1272
16. Bryleva, E. Y., Rogers, M. A., Chang, C. C., Buen, F., Harris, B. T., Rousselet, E., Seidah, N. G., Oddo, S., LaFerla, F. M., Spencer, T. A., Hickey, W. F., and Chang, T. Y. (2010) ACAT1 gene ablation increases 24(S)-hydroxycholesterol content in the brain and ameliorates amyloid pathology in mice with AD. *Proc. Natl. Acad. Sci. U S A* **107**, 3081-3086
17. Hudry, E., Van Dam, D., Kulik, W., De Deyn, P. P., Stet, F. S., Ahouansou, O., Benraiss, A., Delacourte, A., Bougnères, P., Aubourg, P., and Cartier, N. (2010) Adeno-associated virus gene therapy with cholesterol 24-hydroxylase reduces the amyloid pathology before or after the onset of amyloid plaques in mouse models of Alzheimer's disease. *Mol. Ther.* **18**, 44-53
18. Djelti, F., Braudeau, J., Hudry, E., Dhenain, M., Varin, J., Bieche, I., Marquer, C., Chali, F., Ayciriex, S., Auzeil, N., Alves, S., Langui, D., Potier, M. C., Laprevote, O., Vidaud, M., Duyckaerts, C., Miles, R., Aubourg, P., and Cartier, N. (2015) CYP46A1 inhibition, brain cholesterol accumulation and neurodegeneration pave the way for Alzheimer's disease. *Brain* **138**, 2383-2398
19. Chali, F., Djelti, F., Eugene, E., Valderrama, M., Marquer, C., Aubourg, P., Duyckaerts, C., Miles, R., Cartier, N., and Navarro, V. (2015) Inhibiting cholesterol degradation induces neuronal sclerosis and epileptic activity in mouse hippocampus. *Eur. J. Neurosci.* **41**, 1345-1355
20. Mast, N., Andersson, U., Nakayama, K., Björkhem, I., and Pikuleva, I. A. (2004) Expression of human cytochrome P450 46A1 in *Escherichia coli*: effects of N- and C-terminal modifications. *Arch. Biochem. Biophys.* **428**, 99-108
21. Mast, N., White, M. A., Bjorkhem, I., Johnson, E. F., Stout, C. D., and Pikuleva, I. A. (2008) Crystal structures of substrate-bound and substrate-free cytochrome P450 46A1, the principal cholesterol hydroxylase in the brain. *Proc. Natl. Acad. Sci. U S A* **105**, 9546-9551
22. Mast, N., Anderson, K. W., Lin, J. B., Li, Y., Turko, I. V., Tatsuoka, C., Bjorkhem, I., and Pikuleva, I. A. (2017) Cytochrome P450 27A1 deficiency and regional differences in brain sterol metabolism cause preferential cholestanol accumulation in the cerebellum. *J. Biol. Chem.* **292**, 4913-4924
23. Shafaati, M., Mast, N., Beck, O., Nayef, R., Heo, G. Y., Bjorkhem-Bergman, L., Lutjohann, D., Bjorkhem, I., and Pikuleva, I. A. (2010) The antifungal drug voriconazole is an efficient inhibitor of brain cholesterol 24S-hydroxylase (CYP46A1) in vitro and in vivo. *J. Lipid Res.* **51**, 318-323
24. Mast, N., Linger, M., Clark, M., Wiseman, J., Stout, C. D., and Pikuleva, I. A. (2012) *In silico* and intuitive predictions of CYP46A1 inhibition by marketed drugs with subsequent enzyme crystallization in complex with fluvoxamine. *Mol. Pharmacol.* **82**, 824-834
25. Mast, N., Li, Y., Linger, M., Clark, M., Wiseman, J., and Pikuleva, I. A. (2014) Pharmacologic stimulation of cytochrome P450 46A1 and cerebral cholesterol turnover in mice. *J. Biol. Chem.* **289**, 3529-3538
26. Mast, N., Liao, W. L., Pikuleva, I. A., and Turko, I. V. (2009) Combined use of mass spectrometry and heterologous expression for identification of membrane-interacting peptides in cytochrome P450 46A1 and NADPH-cytochrome P450 oxidoreductase. *Arch. Biochem. Biophys.* **483**, 81-89
27. Mast, N., Charvet, C., Pikuleva, I. A., and Stout, C. D. (2010) Structural basis of drug binding to CYP46A1, an enzyme that controls cholesterol turnover in the brain. *J. Biol. Chem.* **285**, 31783-31795
28. Mast, N., Zheng, W., Stout, C. D., and Pikuleva, I. A. (2013) Antifungal azoles: structural insights into undesired tight binding to cholesterol-metabolizing CYP46A1. *Mol. Pharmacol.* **84**, 86-94
29. Mast, N., Zheng, W., Stout, C. D., and Pikuleva, I. A. (2013) Binding of a cyano- and fluoro-containing drug bicalutamide to cytochrome P450 46A1: Unusual features and spectral response. *J. Biol. Chem.* **288**, 4613-4624

30. Anderson, K. W., Mast, N., Hudgens, J. W., Lin, J. B., Turko, I. V., and Pikuleva, I. A. (2016) Mapping of the allosteric site in cholesterol hydroxylase CYP46A1 for efavirenz, a drug that stimulates enzyme activity. *J. Biol. Chem.* **291**, 11876-11886
31. Bretillon, L., Lutjohann, D., Stahle, L., Widhe, T., Bindl, L., Eggertsen, G., Diczfalusy, U., and Björkhem, I. (2000) Plasma levels of 24S-hydroxycholesterol reflect the balance between cerebral production and hepatic metabolism and are inversely related to body surface. *J. Lipid Res.* **41**, 840-845
32. Ohyama, Y., Meaney, S., Heverin, M., Ekstrom, L., Brafman, A., Shafir, M., Andersson, U., Olin, M., Eggertsen, G., Diczfalusy, U., Feinstein, E., and Björkhem, I. (2006) Studies on the transcriptional regulation of cholesterol 24-hydroxylase (CYP46A1): marked insensitivity toward different regulatory axes. *J. Biol. Chem.* **281**, 3810-3820
33. Shafaati, M., O'Driscoll, R., Björkhem, I., and Meaney, S. (2009) Transcriptional regulation of cholesterol 24-hydroxylase by histone deacetylase inhibitors. *Biochem. Biophys. Res. Commun.* **378**, 689-694
34. Milagre, I., Nunes, M. J., Moutinho, M., Rivera, I., Fuso, A., Scarpa, S., Gama, M. J., and Rodrigues, E. (2010) Chromatin-modifying agents increase transcription of CYP46A1, a key player in brain cholesterol elimination. *J. Alzheimers Dis.* **22**, 1209-1221
35. Nunes, M. J., Milagre, I., Schneckeburger, M., Gama, M. J., Diederich, M., and Rodrigues, E. (2010) Sp proteins play a critical role in histone deacetylase inhibitor-mediated derepression of CYP46A1 gene transcription. *J. Neurochem.* **113**, 418-431
36. Milagre, I., Nunes, M. J., Gama, M. J., Silva, R. F., Pascussi, J. M., Lechner, M. C., and Rodrigues, E. (2008) Transcriptional regulation of the human CYP46A1 brain-specific expression by Sp transcription factors. *J. Neurochem.* **106**, 835-449
37. Sodero, A. O., Vriens, J., Ghosh, D., Stegner, D., Brachet, A., Pallotto, M., Sassoe-Pognetto, M., Brouwers, J. F., Helms, J. B., Nieswandt, B., Voets, T., and Dotti, C. G. (2012) Cholesterol loss during glutamate-mediated excitotoxicity. *EMBO J.* **31**, 1764-1773
38. Emnett, C. M., Eisenman, L. N., Mohan, J., Taylor, A. A., Doherty, J. J., Paul, S. M., Zorumski, C. F., and Mennerick, S. (2015) Interaction between positive allosteric modulators and trapping blockers of the NMDA receptor channel. *Br. J. Pharmacol.* **172**, 1333-1347
39. Meldrum, B. S. (2000) Glutamate as a neurotransmitter in the brain: review of physiology and pathology. *J. Nutr. Biochem.* **130**, 1007S-1015S
40. Featherstone, D. E. (2010) Intercellular glutamate signaling in the nervous system and beyond. *ACS Chem. Neurosci.* **1**, 4-12
41. Poulos, T. L., Finzel, B. C., and Howard, A. J. (1986) Crystal structure of substrate-free *Pseudomonas putida* cytochrome P-450. *Biochemistry* **25**, 5314-5322
42. Remmer, H., Schenkman, J., Estabrook, R. W., Sasame, H., Gillette, J., Narasimhulu, S., Cooper, D. Y., and Rosenthal, O. (1966) Drug interaction with hepatic microsomal cytochrome. *Mol. Pharmacol.* **2**, 187-190
43. Schenkman, J. B., Remmer, H., and Estabrook, R. W. (1967) Spectral studies of drug interaction with hepatic microsomal cytochrome. *Mol. Pharmacol.* **3**, 113-123
44. Guengerich, F. P., and Johnson, W. W. (1997) Kinetics of ferric cytochrome P450 reduction by NADPH-cytochrome P450 reductase: Rapid reduction in the absence of substrate and variations among cytochrome P450 systems. *Biochemistry* **36**, 14741-14750
45. Linsensbardt, A. J., Taylor, A., Emnett, C. M., Doherty, J. J., Krishnan, K., Covey, D. F., Paul, S. M., Zorumski, C. F., and Mennerick, S. (2014) Different oxysterols have opposing actions at N-methyl-D-aspartate receptors. *Neuropharmacology* **85**, 232-242
46. Meaney, S., Bodin, K., Diczfalusy, U., and Björkhem, I. (2002) On the rate of translocation in vitro and kinetics in vivo of the major oxysterols in human circulation: critical importance of the position of the oxygen function. *J. Lipid Res.* **43**, 2130-2135



47. White, M. A., Mast, N., Björkhem, I., Johnson, E. F., Stout, C. D., and Pikuleva, I. A. (2008) Use of complementary cation and anion heavy-atom salt derivatives to solve the structure of cytochrome P450 46A1. *Acta Crystallogr. D Biol. Crystallogr.* **64**, 487-495
48. Hanna, I. H., Teiber, J. F., Kokones, K. L., and Hollenberg, P. F. (1998) Role of the alanine at position 363 of cytochrome P450 2B2 in influencing the NADPH- and hydroperoxide-supported activities. *Arch. Biochem. Biophys.* **350**, 324-332
49. Mast, N., Reem, R., Bederman, I., Huang, S., DiPatre, P. L., Björkhem, I., and Pikuleva, I. A. (2011) Cholestenoic acid is an important elimination product of cholesterol in the retina: comparison of retinal cholesterol metabolism with that in the brain. *Invest. Ophthalmol. Vis. Sci.* **52**, 594-603
50. Burleigh, B. D., Jr., Foust, G. P., and Williams, C. H., Jr. (1969) A method for titrating oxygen-sensitive organic redox systems with reducing agents in solution. *Anal. Biochem.* **27**, 536-544
51. Foust, G. P., Burleigh, B. D., Jr., Mayhew, S. G., Williams, C. H., Jr., and Massey, V. (1969) An anaerobic titration assembly for spectrophotometric use. *Anal. Biochem.* **27**, 530-535
52. Guengerich, F. P., Krauser, J. A., and Johnson, W. W. (2004) Rate-limiting steps in oxidations catalyzed by rabbit cytochrome P450 1A2. *Biochemistry* **43**, 10775-10788
53. Patil, P. V., and Ballou, D. P. (2000) The use of protocatechuate dioxygenase for maintaining anaerobic conditions in biochemical experiments. *Anal. Biochem.* **286**, 187-192
54. Palfey, B. A. (2003) Time resolved spectral analysis, in *Kinetic Analysis of Macromolecules* (Johnson, K. A., ed.), Oxford University Press, New York. pp 203-228
55. Daniels, F., and Alberty, R. A. (1966), in *Physical Chemistry*, 3<sup>rd</sup> Ed., John Wiley & Sons, New York. pp 336-338
56. Pascal, B. D., Willis, S., Lauer, J. L., Landgraf, R. R., West, G. M., Marciano, D., Novick, S., Goswami, D., Chalmers, M. J., and Griffin, P. R. (2012) HDX workbench: Software for the analysis of H/D exchange MS data. *J. Am. Soc. Mass. Spectrom.* **23**, 1512-1521
57. Zhang, Z., and Smith, D. L. (1993) Determination of amide hydrogen exchange by mass spectrometry: a new tool for protein structure elucidation. *Protein Sci.* **2**, 522-531
58. Grosdidier, A., Zoete, V., and Michielin, O. (2011) SwissDock, a protein-small molecule docking web service based on EADock DSS. *Nucleic Acids Res.* **39**, W270-277

Table 1. Rates of Reduction of Ferric CYP46A1 by OR Under Various Conditions

Additive	“Fast”, phase 1 (0-2 s)		“Slow”, phase 2 (2-60 s)		Total P450 reduced, $\mu\text{M}$	Total P450, $\mu\text{M}$	% Phase 1/phase 2 reduction	% Total P450 reduced,
	$k_1$ , $\text{s}^{-1}$	P450 reduced, $\mu\text{M}$	$k_2$ , $\text{s}^{-1}$	P450 reduced, $\mu\text{M}$				
None	0.96±0.27 (n = 17)	0.12±0.04 (n = 18)	0.060±0.004 (n = 17)	0.15±0.04 (n = 18)	0.27	0.9 <sup>a</sup>	44/56	30
Cholesterol <sup>b</sup>	1.26±0.13 (n = 17)	0.26±0.02 (n = 7)	0.060±0.003 (n = 7)	0.37±0.01 (n = 7)	0.63	1.5 <sup>c</sup>	41/59	42
L-Glu	0.96±0.23 (n = 14)	0.26±0.05 (n = 14)	0.062±0.003 (n = 10)	0.42±0.05 (n = 10)	0.68	1.5	38/62	45
L-Glu, Cholesterol <sup>b,d,e</sup>	1.45±0.11 (n = 16)	0.34±0.06 (n = 17)	0.058±0.002 (n = 8)	0.40±0.03 (n = 7)	0.74	1.5	46/54	50
EFV	1.12±0.05 (n = 4)	0.46±0.02 (n = 4)	0.065±0.006 (n = 3)	0.50±0.01 (n = 3)	0.96	1.5 <sup>c</sup>	48/52	64
EFV, Cholesterol <sup>b,d,e</sup>	1.39±0.10 (n = 15)	0.47±0.05 (n = 16)	0.057±0.002 (n = 3)	0.21±0.09 (n = 3)	0.68	1.5	69/31	45
EFV, L-Glu, Cholesterol <sup>b</sup>	1.31±0.06 (n = 8)	0.55±0.3 (n = 8)	0.063±0.003 (n = 6)	0.49±0.02 (n = 6)	1.04	1.5	53/47	69

<sup>a</sup>P450 loss during degassing. In a control experiment we determined that the residual P450 concentration would have been 0.9  $\mu\text{M}$ .

<sup>b</sup>A statistically significant change in  $k_1$  ( $p \leq 0.05$ ) as compared to CYP46A1 with no additives.

<sup>c</sup>No P450 loss during degassing.

<sup>d</sup>A statistically significant change in  $k_1$  ( $p \leq 0.05$ ) as compared to CYP46A1 incubations with cholesterol.

<sup>e</sup>A statistically significant change in  $k_1$  ( $p \leq 0.05$ ) as compared to CYP46A1 incubations with the corresponding activator.

## Footnotes:

This work was supported in part by United States Public Health Service Grants R01 GM062882 (to I.A.P), P30 Core Grant EY011373, and R01 GM118122 (to F.P.G.). The authors declare no competing financial interest with the contents of this article. Certain commercial materials, instruments, and equipment are identified in this manuscript in order to specify the experimental procedure as completely as possible. In no case does such identification imply a recommendation or endorsement by the National Institute of Standards and Technology nor does it imply that the materials, instruments, or equipment identified are necessarily the best available for the purpose. The content is solely the responsibility of the authors and does not necessarily represent the official views of the National Institutes of Health.

The abbreviations used are: Ach, acetylcholine; CYP or P450, cytochrome P450; EFV, efavirenz; GABA,  $\gamma$ -aminobutyric acid; Glu, D- or L-isomer of glutamate; 24HC, 24(S)-hydroxycholesterol; HDX, hydrogen-deuterium exchange; NMDA, N-methyl-D-aspartate; OR, NADPH-cytochrome P450 oxidoreductase.

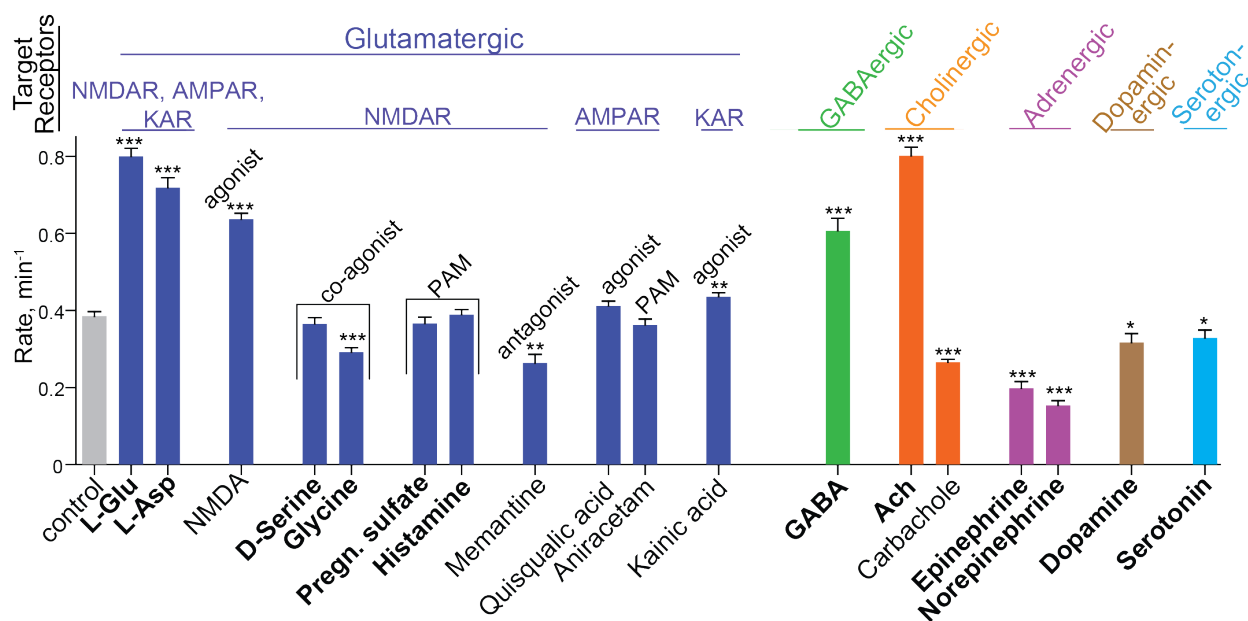


**FIGURE 1. Effect of neuroactive compounds on CYP46A1 activity *in vitro*.** The conditions of the screening enzyme assay are described under “Experimental Procedures.”  $\Delta(2-50)$ CYP46A1 ( $0.5 \mu\text{M}$ ) was used; the cholesterol and neuroactive compound concentrations were  $40 \mu\text{M}$  and  $20 \mu\text{M}$ , respectively. The amount of 24-hydroxycholesterol formed was determined by gas chromatography-mass spectrometry. The rates of cholesterol 24-hydroxylation activity of CYP46A1 represent nmol of 24-hydroxycholesterol formed per nmol of CYP46A1 per min. The results are presented as means  $\pm$  S.D. of measurements from three independent experiments. Control incubations contained no neuroactive compound. Neurotransmitters are in bold and exogenous neuroactive compounds are in regular font. NMDAR, AMPAR, and KAR, receptors for *N*-methyl-D-aspartate,  $\alpha$ -amino-3-hydroxy-5-methyl-4-isoxazolepropionic, and kainic acids, respectively. L-Glu, L-glutamate; L-Asp, L-aspartate; NMDA, N-methyl-D-aspartate; PAM, positive allosteric modulator; GABA,  $\gamma$ -aminobutyric acid; Ach, acetylcholine. \*,  $p \leq 0.05$ ; \*\*,  $p \leq 0.01$ ; \*\*\*,  $p \leq 0.001$  by a two-tailed unpaired Student’s *t*-test as compared to control incubations.



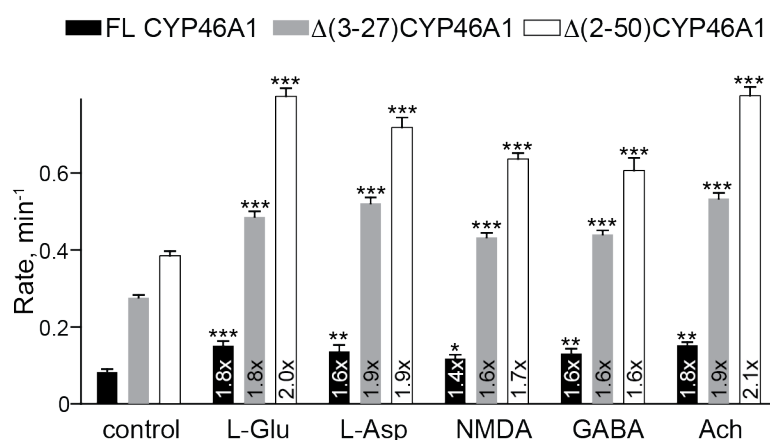


**FIGURE 2. Effect of truncation on CYP46A1 activation by neuroactive compounds.** The assay conditions are described under “Experimental Procedures.” The P450 concentration was 0.5  $\mu\text{M}$ ; the cholesterol and neuroactive compound concentrations were 40 and 20  $\mu\text{M}$ , respectively; incubations with full-length CYP46A1 contained 0.02% CYMAL-6 (w/v). The results are presented as means  $\pm$  S.D. of the measurements from three independent experiments. FL, full-length CYP46A1 (*black bars*),  $\Delta(3-27)$ CYP46A1 (*gray bars*), and  $\Delta(2-50)$ CYP46A1 (*open bars*). Numbers inside the bars indicate a fold of CYP46A1 activation as compared to control incubations with no activator. The abbreviations, units of CYP46A1 activity, statistical analysis as well as *p* values are the same as in Fig. 1.

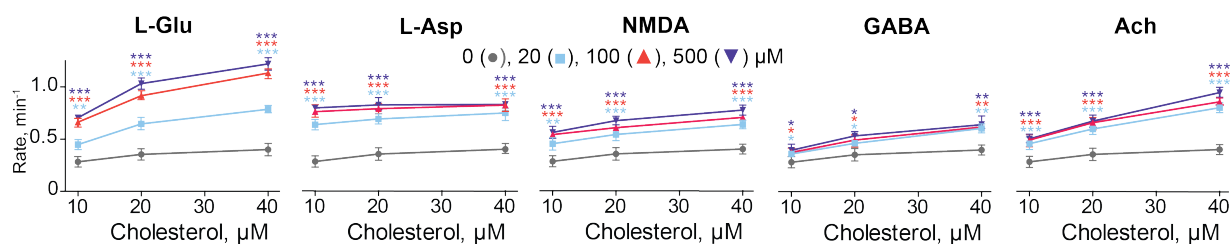


**FIGURE 3. Effect of varying cholesterol and neuroactive compound concentrations on CYP46A1 activation *in vitro*.** The assay conditions are described under “Experimental Procedures.”  $\Delta(2-50)$ CYP46A1 ( $0.5 \mu\text{M}$ ) was used; the concentrations of cholesterol were 10, 20, and  $40 \mu\text{M}$ , and those of the indicated neuroactive compounds were 20, 100, and  $500 \mu\text{M}$ . The results are presented as means  $\pm$  S.D. of the measurements from three independent experiments. Control incubations (*gray lines*) contained no neuroactive compound. The abbreviations, units of CYP46A1 activity, and *p* values are the same as in Fig. 1. Light blue, red, and dark blue asterisks represent significant changes as compared to incubations with no neuroactive compound by repeated measures two-way ANOVA followed by a *post hoc* Bonferroni multiple comparison test.

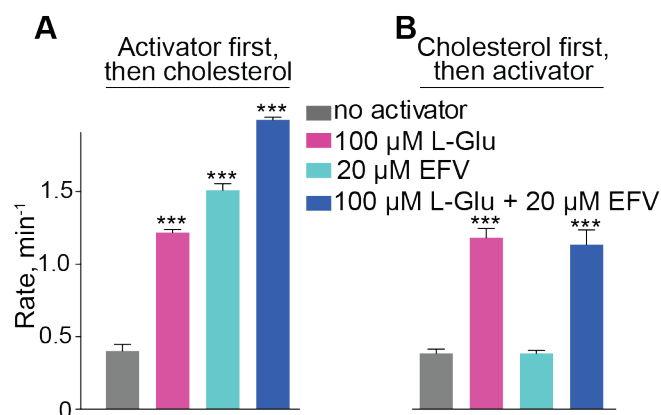


**FIGURE 4. Effect of the order of reagent mixing on CYP46A1 activation by L-Glu (magenta bars).** Experiments with efavirenz (EFV, cyan bars), another CYP46A1 activator, are shown for comparison. Control incubations contained no activator and are shown as gray bars. The assay conditions are described under “Experimental Procedures.” *A*, the reagents were mixed in the following order. First, chilled 50 mM KP<sub>i</sub> buffer (pH 7.2) containing 100 mM NaCl was added to the tube placed on ice. Then 100 μM L-Glu or 20 μM EFV was added and mixed with the buffer. Next, 0.5 μM Δ(2-50)CYP46A1 was added and gently mixed followed by addition of 1 μM NADPH-cytochrome P450 oxidoreductase and 2 U catalase. Finally, 40 μM cholesterol was added, and the tube was transferred to a water bath maintained at 37 °C. Enzymatic reaction was initiated with the addition of 1 mM NADPH. *B*, the reagents were mixed like in panel *A*, except the addition of activator and cholesterol was swapped. The results are presented as means ± S.D. of the measurements from three independent experiments. The abbreviations, units of CYP46A1 activity, and *p* values are the same as in Fig. 1.

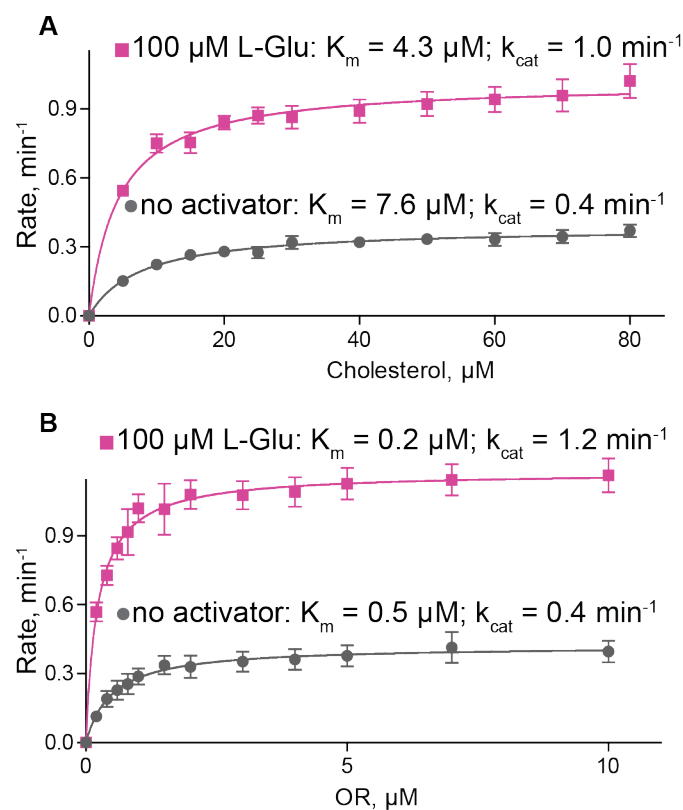


**FIGURE 5. Effect of L-Glu on  $\Delta(2-50)\text{CYP46A1}$  kinetic properties.** *A* and *B*, rates of cholesterol 24-hydroxylation *versus* increasing cholesterol and NADPH-cytochrome P450 oxidoreductase (OR) concentrations, respectively, in the absence (*gray lines*) and presence (*magenta lines*) of 100  $\mu\text{M}$  L-Glu. Control incubations contained no neuroactive compound. The data were fit to the Michaelis-Menten equation with hyperbolic fitting and non-linear regression. Representative curves are shown. The results are presented as means  $\pm$  S.D. of triplicate measurements. The abbreviations and units of CYP46A1 activity, are the same as in Fig. 1. The assay conditions are described under “Experimental Procedures.”



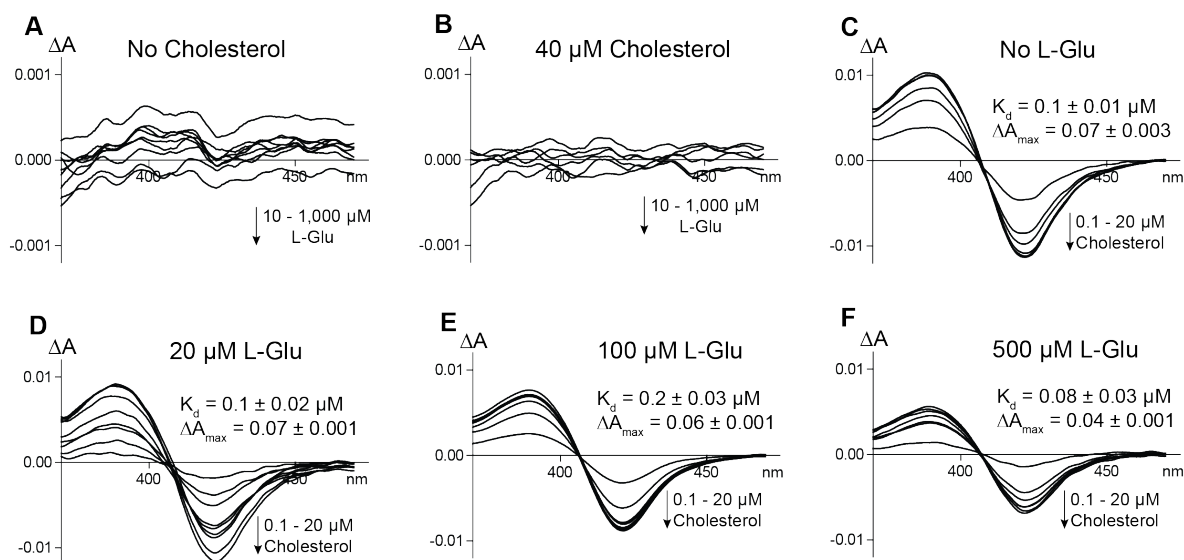


**FIGURE 6. Effect of L-Glu on spectral properties of CYP46A1.** The assay conditions are described under “Experimental Procedures.” Different  $\Delta(2-50)$ CYP46A1 solutions (0.3  $\mu M$ ) were prepared: in the absence of cholesterol (*A*) and L-Glu (*C*) and in the presence of 40  $\mu M$  cholesterol (*B*) and 20, 100, and 500  $\mu M$  L-Glu (*D-F*). These solutions were placed in cuvettes (equal volumes, 1 ml) in the sample and reference chambers of a spectrophotometer and titrated with either L-Glu (10-1,000  $\mu M$ , *A* and *B*) or cholesterol (0.1-20  $\mu M$ , *C-F*). Spectral responses represent the difference of the absorbance ( $\Delta A$ ) in a sample cuvette containing CYP46A1 and increasing amounts of either L-Glu or cholesterol vs the absorbance in a reference cuvette containing CYP46A1 and increasing amounts of the solvent, in which L-Glu or cholesterol were dissolved. The results are presented as means  $\pm$  S.D. of the measurements from three independent experiments. The abbreviations are the same as in Fig. 1.

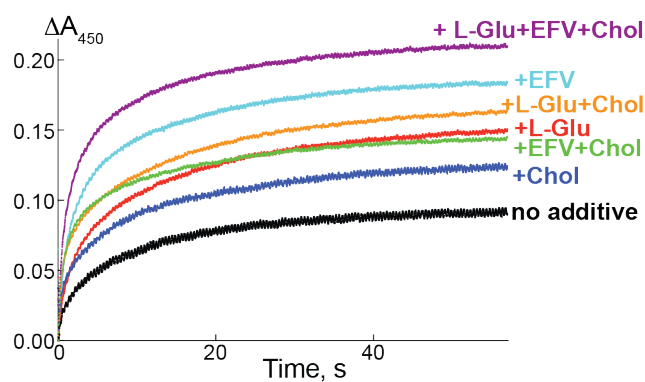


**FIGURE 7. The kinetics of ferric  $\Delta(2-50)$ CYP46A1 reduction by NADPH-cytochrome P450 oxidoreductase under different conditions.** Representative traces are shown. The assay conditions are described under “Experimental Procedures.” The rates of P450 reduction and amount of reduced P450 were measured in a stopped-flow spectrophotometer by trapping the ferrous enzyme in an anaerobic environment as the complex with CO. Assays were done by mixing the contents of two syringes. One syringe contained (among other reagents) 3  $\mu$ M  $\Delta(2-50)$ CYP46A and 6  $\mu$ M OR; cholesterol (40  $\mu$ M), L-Glu (100  $\mu$ M), and EFV (20  $\mu$ M) were added as noted. The other syringe contained (among other reagents) 0.40 mM NADPH. The abbreviations are the same as in Figs. 1 and 4.

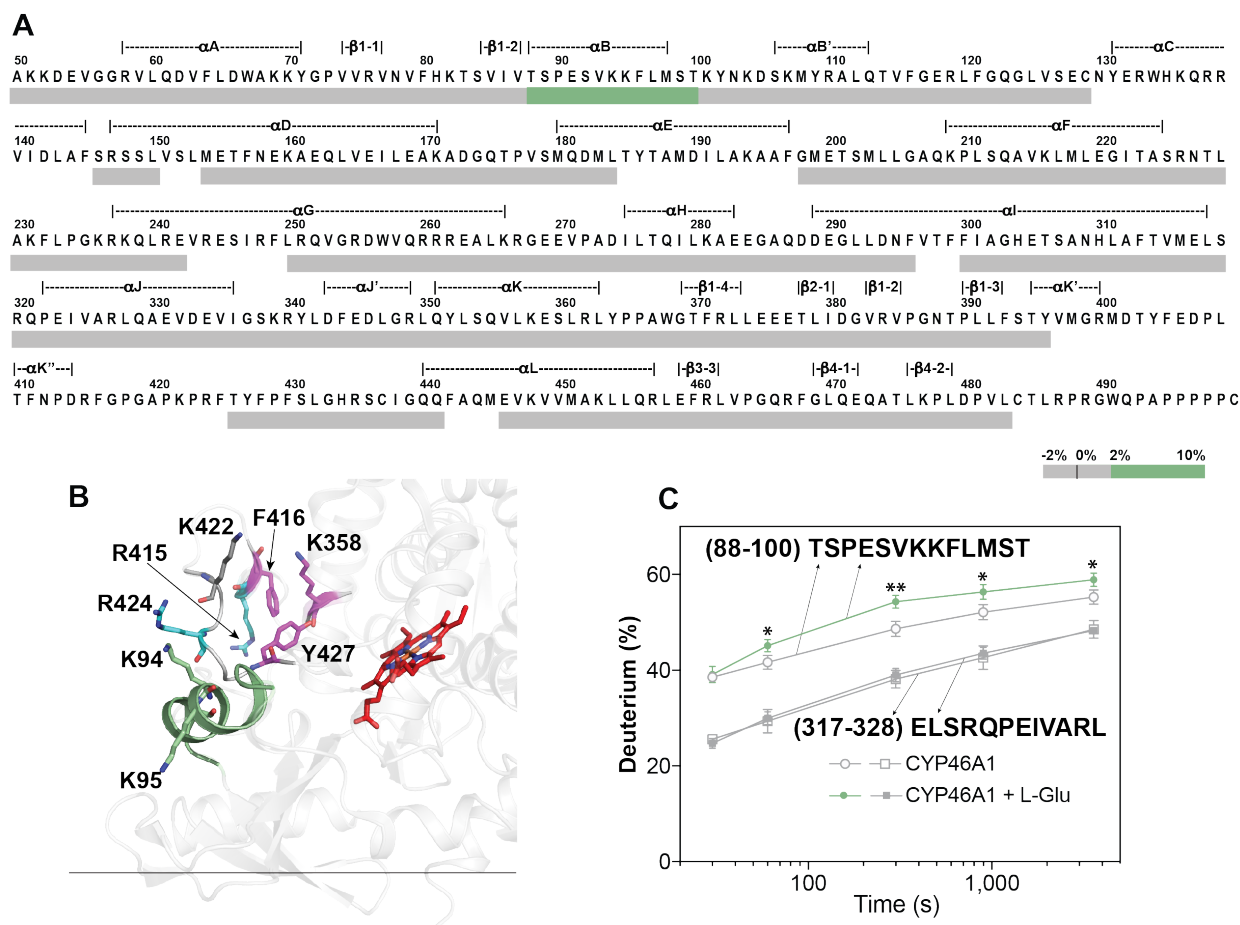


**FIGURE 8. Differential HDX analysis for the L-Glu-bound CYP46A1 versus L-Glu-free CYP46A1.** The details of this assay are described under “Experimental Procedures.” In-brief, two samples of  $\Delta(2-50)$ CYP46A1, in the absence and presence of 100  $\mu$ M L-Glu, were diluted in the  $D_2O$  buffer following incubation for 15 min at room temperature in undeuterated buffer. HDX was then performed for 30 s, 1 min, 5 min, 15 min, and 1 h exchange times at 25 °C, and exchange reactions were quenched by addition of 3 M urea and 100 mM sodium phosphate (pH 2.5) and lowering the solution temperature to 1 °C. CYP46A1 was then digested on an immobilized pepsin column. The peptides obtained were separated and analyzed by LC-MS and identified using MASCOT software. The difference in deuterium uptake ( $\Delta D\%$ ) for each peptide pair in the L-Glu-free and L-Glu-bound CYP46A1 was calculated by subtracting the difference between the mean  $D\%$  values (representing the average of all time points) for the peptides. The significances in  $\Delta D\%$  ( $p < 0.05$ ) were then established by paired t-tests (HDX Workbench), and differential HDX maps were generated by consolidating peptide-level information into single, linear amino acid sequence and showing only the regions with the statistically significant differences. *A*, colored bar mapping of the consolidated regions with no change (gray) and increased (green) deuterium uptake in the CYP46A1 primary sequence. The color code is shown at the bottom. The dashed lines above the CYP46A1 primary sequence indicate the protein secondary structural elements. *B*, mapping of the region with increased deuterium uptake and the two positively side chains in this region (all are in green) on the CYP46A1 crystal structure (PDB code 2Q9G). The heme is in red. The nitrogen and oxygen atoms are in blue and red, respectively. The side chains of amino acid residues tested for the involvement in L-Glu and EFV binding are in magenta and cyan, respectively. The side chain of K422 (in gray) is also shown. The black horizontal line separates the cytosolic (above) and membrane-associated (below) portions of CYP46A1. *C*, kinetics of deuterium incorporation in the Thr-88/Thr-100 CYP46A1 peptide that showed significant differences between the L-Glu-bound CYP46A1 (green) and L-Glu-free CYP46A1 (gray). A surface CYP46A1 peptide (Glu-317-Leu-328) that did not show any difference in deuterium uptake between the two P450 samples is shown for comparison. The results are presented as means  $\pm$  SD of triplicate measurements. The abbreviations, statistical analysis as well as  $p$  values are the same as in Fig. 1.

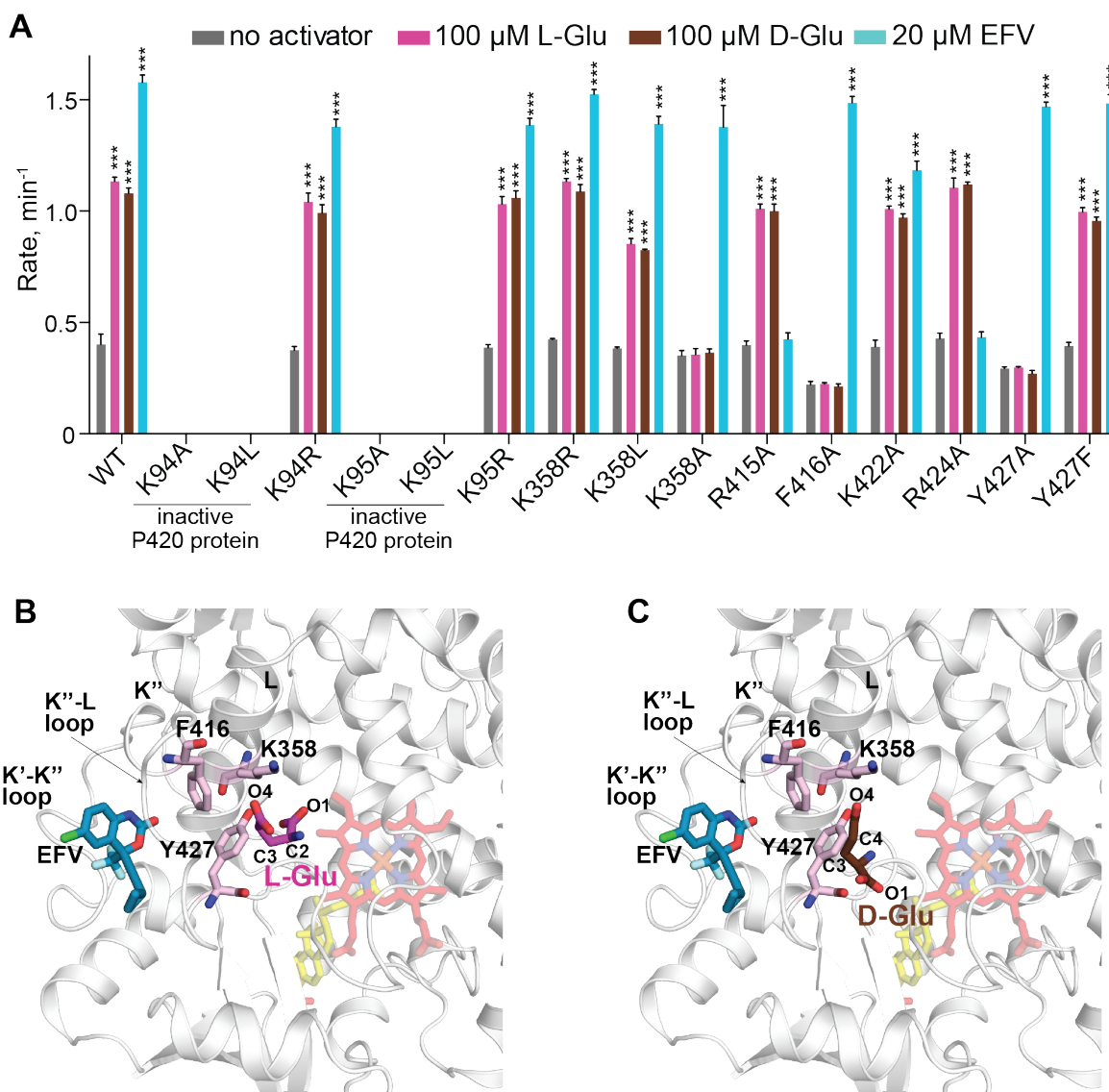


**FIGURE 9. Mapping of the CYP46A1 site for Glu binding.** *A*, effect of mutations on  $\Delta(2-50)$ CYP46A1 activation by 100  $\mu$ M L-Glu (magenta bars), 100  $\mu$ M D-Glu (brown bars), and 20  $\mu$ M EFV (cyan bars).  $\Delta(2-50)$ CYP46A1 basal activity (no activator) is shown as gray bars. The assay conditions are described under “Experimental Procedures;” the cholesterol concentration was 40  $\mu$ M. The results are presented as means  $\pm$  S.D. of the measurements from three independent experiments. The abbreviations, units of CYP46A1 activity, statistical analysis as well as *p* values are the same as in Figs. 1 and 4. *B*, computational models of L-Glu (magenta) and EFV (dark cyan) binding, respectively, to cholesterol sulfate-bound CYP46A1 (PDB code 2Q9F). *C*, a computational model of D-Glu (brown) binding to cholesterol sulfate-bound CYP46A1 (PDB code 2Q9F). The color code is the same as in Fig. 8. The molecule of cholesterol sulfate is in yellow.



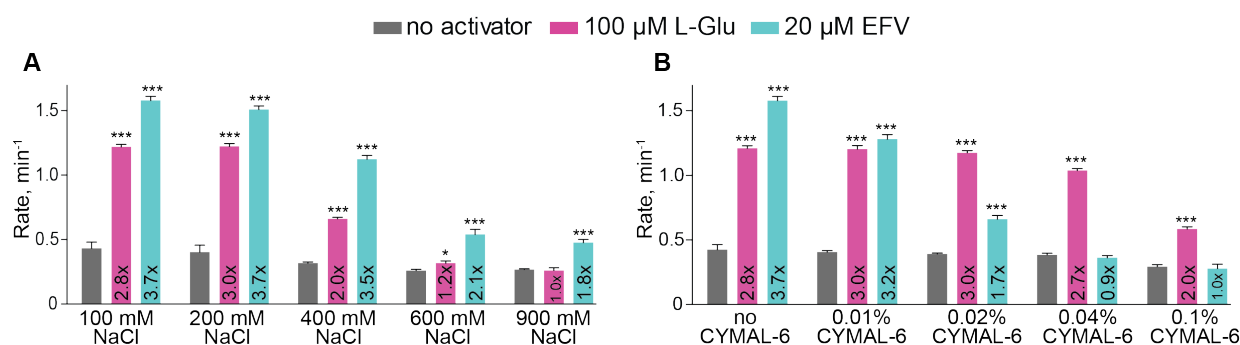


**FIGURE 10. L-Glu and EFV interactions with CYP46A1.** *A* and *B*, effects of ionic strength and hydrophobic interactions on  $\Delta(2-50)$ CYP46A1 activation by L-Glu (magenta bars) and EFV (cyan bars), respectively. Control incubation (no activator) are shown as gray bars. Numbers inside the bars indicate a fold of CYP46A1 activation as compared to control incubations with no activator present. The assay conditions were the same as in the screening assay (described under “Experimental Procedures”) including the concentration of  $\Delta(2-50)$ CYP46A1 (0.5  $\mu$ M) and cholesterol (40  $\mu$ M). The only exception was the concentration of L-Glu, which was higher and equal to 100  $\mu$ M. The results are presented as means  $\pm$  S.D. of the measurements from three independent experiments. The abbreviations, units of CYP46A1 activity, statistical analysis as well as *p* values are the same as in Figs. 1 and 4.

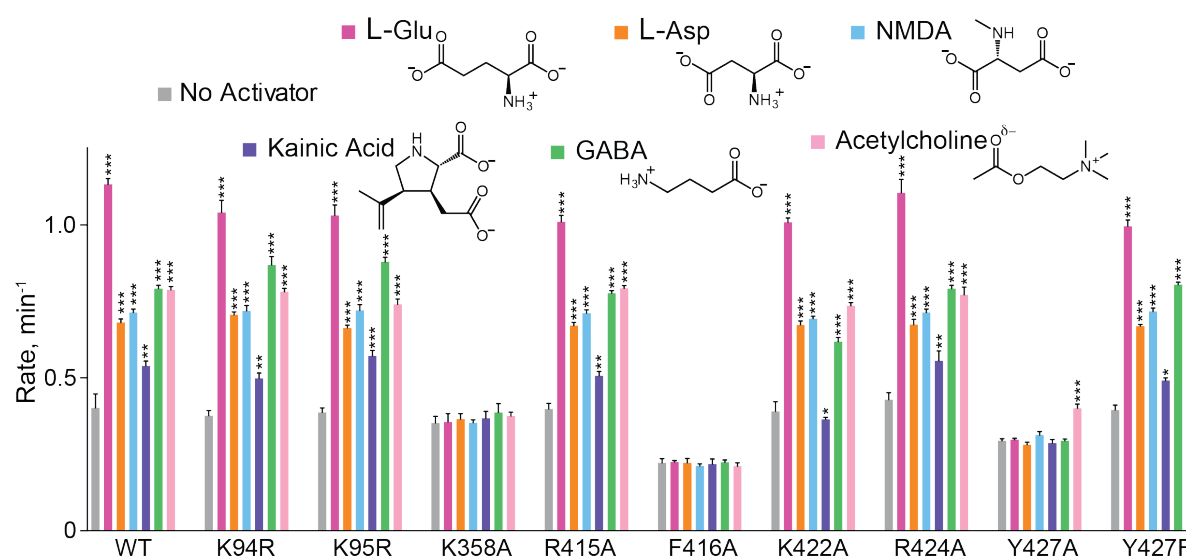


**FIGURE 11. Effect of mutations on CYP46A1 activation by different neuroactive compounds.** Control incubations (no activator) are shown as *gray* bars and activity in the presence of neuroactive compounds as colored bars. The structure and color code for each neuroactive compound are at the top. The assay conditions are described under “Experimental Procedures.”  $\Delta(2-50)$ CYP46A1 ( $0.5 \mu\text{M}$ ) was used; the cholesterol and neuroactive compound concentrations were  $40 \mu\text{M}$  and  $100 \mu\text{M}$ , respectively. The results are presented as means  $\pm$  S.D. of the measurements from three independent experiments. The abbreviations, statistical analysis as well as *p* values are the same as in Fig. 1.

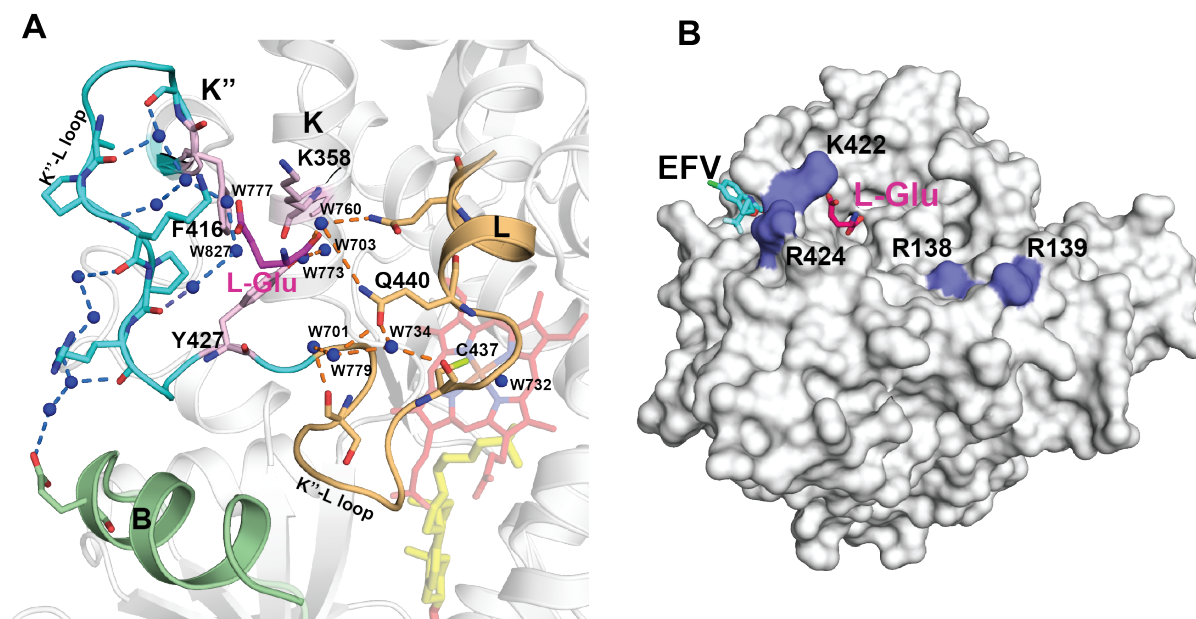


FIGURE 12. **Possible mechanisms mediating L-Glu effects.** *A*, water molecules (*blue spheres*) and amino acid residues involved in signal transduction from the CYP46A1 allosteric site to the proximal part of the CYP46A1 active site. Two hydrogen bond networks are shown, one (*in cyan and blue*) is linked to the B helix showing an increase in deuterium uptake upon L-Glu binding, and the other one (*in wheat and orange*) is linked to C437 serving as the fifth heme iron ligand. The remaining of the color code is the same as in Figs. 8 and 9. Dashed lines of blue and orange colors represent hydrogen bonds in two different networks. *B*, surface representation of the CYP46A1 molecule showing L-Glu positioning in the trough of the site involved in OR binding. Residues involved in the interaction with OR are in blue. EFV binding is also shown. The abbreviations and color code are the same as in Figs. 1, 4, 5, 8, and 9.

***In vitro* cytochrome P450 46A1 (CYP46A1) activation by neuroactive compounds**  
Natalia Mast, Kyle W. Anderson, Kevin M. Johnson, Thanh T.N. Phan, F. Peter Guengerich  
and Irina A. Pikuleva

*J. Biol. Chem.* published online June 22, 2017

---

Access the most updated version of this article at doi: [10.1074/jbc.M117.794909](https://doi.org/10.1074/jbc.M117.794909)

Alerts:

- [When this article is cited](#)
- [When a correction for this article is posted](#)

[Click here](#) to choose from all of JBC's e-mail alerts

This article cites 0 references, 0 of which can be accessed free at  
<http://www.jbc.org/content/early/2017/06/22/jbc.M117.794909.full.html#ref-list-1>